*The paper was published in the proceedings of the 7th International Conference on Earthquake Geotechnical Engineering and was edited by Francesco Silvestri, Nicola Moraci and Susanna Antonielli. The conference was held in Rome, Italy, 17 – 20 June 2019.*

*Earthquake Geotechnical Engineering for Protection and Development of Environment and Constructions – Silvestri & Moraci (Eds)*
 *ISBN 978-0-367-14328-2*

# Genetic algorithm framework for *p-y* curve derivation

C. Favaretti
*Arup, New York, New York, USA*

N.J. Ceglia
*Memorial Sloan Kettering, New York, New York, USA*

A. Lemnitzer
*University of California at Irvine, Irvine, California, USA*

ABSTRACT: Subgrade reaction methods, as implemented through the *p-y* curve analysis, remain the most globally utilized analytical tool to characterize the lateral response of deep foundations. As recognized by many researchers, traditional procedures are known pose challenges in obtaining suitable data fits, or mathematical difficulties associated with data differentiation. The results obtained from a model-scale lateral loaded test on a concrete pile in sand are presented and analyzed through an optimization technique. A genetic algorithm framework is developed to facilitate data interpretation in presence of disturbed data readings and pile nonlinearity. This approach overcomes existing challenges affecting the experimental derivation of *p-y* curves (e.g. choice of fitting technique and input parameters) by using an ensemble of statistical methods and minimizing an objective fitness function. Experimentally derived *p-y* curves are then compared with traditional analytical models found in literature.

## 1 INTRODUCTION

Current *p-y* curves recommendations, as assembled within the guidelines of the American Petroleum Institute API (2000), refer to pioneering experimental studies on small diameter (0.6 m) piles (e.g. Matlock (1970) and Reese & Welch (1975)). Over the past decades, significant research contributions in the field of *p-y* formulations have been made and provide more specific knowledge on issues such as nonlinear performance behavior and pile boundary conditions (e.g. pile diameter effect, installation techniques, head and tip fixity,*p-y* and *t-z* coupling effects). Since their original development, new types of pile foundations (e.g. pile groups, micro piles, large-diameter drilled shafts, driven and battered piles, or drilled displacement piles) have been constructed and require design recommendations that are extrapolate-able to their specific soil-struc- ture conditions. Many researchers have documented the challenges associated with deriving new *p-y* relationships for the vast variety of pile configurations in practice (e.g. de Sousa Countinho (2006), Yang & Liang (2006), Brandenberg et al. (2010)), particularly with respect to curve fitting of curvature and strain data, as well as double differentiation and integration processes.

This paper presents a small-scale pile testing program in medium-dense dry sand and serves as pilot data platform for the development of a genetic algorithm framework that is used to derive *p-y* from experimental test data. The instrumented pile specimen was subjected to quasi-static lateral loading, and *p-y* curves were then derived following the classical derivation method, optimized in a genetic algorithm framework. Experimentally derived *p-y* curves are compared with traditional *p-y* curve formulations from literature.

## 2 TEST PROGRAM

### 2.1 *Experimental setup and material properties*

The pile test presented in this paper is part of a four pile test series on reinforced concrete piles with different boundary conditions, reinforcement scenarios, and pile diameters. The pile selected for this publication consisted of a 20 cm diameter reinforced concrete pile with a total length of 3.0 m. The pile was constructed as model-scale column specimen and placed in a laminar soil box with dimensions of 1.8 m in length, 1.0 m in width and 2.4 m in height. The laminar box consisted of 19 aluminum frames, with a 0.5 m thickness, separated by steel rollers with a 14 cm diameter (Figure 1(a)). During testing, the box was restrained using a rigid bracing system, consisting of concrete reaction blocks, wooden braces and steel girders. The movement of the box was monitored during testing and deformations were found to be negligible.

The fill material consisted of commercially available sand named #16 Industrial Sand (Supplier: P.W. Gillibrand). The material is a clean, washed, and fine sand, classified as poorly graded. The specific gravity of solids (Gs) was determined to be 2.63 (ASTM D854). Modified Proctor Compaction testing revealed a maximum dry unit weight ($\gamma_{max}$) of 18.8 kN/m at an optimum water content of 11% (ASTM D1557). The minimum dry unit weight ($\gamma_{min}$) was 14 $kN/m^3$ (ASTM D4254). Direct shear testing yielded a friction angle, $\phi$, of 44° with an average cohesion, *c,* of 5 $kN/m^2$ (ASTM D3080).

The dry pluviation technique was used to place the sand into the laminar soil box. A pluviator was designed, constructed, and calibrated for this application. The pluviator consisted of a wooden hopper (W= 0.75 m, L= 1 m, and H= 0.9 m), with a 20 cm hole in the center, which could be opened and closed through a valve. The device was moved during the pluviation process by a three-axis crane to serve the entire surface of the laminar soil box. The calibration procedure considered the influence of falling height, valve aperture size, and flow rate on the achievable relative density, DR. The calibration tests showed that the relative density of the sand was stronger influenced by the flow rate rather than the drop height. Therefore, the mass flux was controlled using a No.6 sieve at the bottom opening of the pluviation box, which enabled a uniform flow rate of 65 $cm^3$/sec. Sample measurements during the placement process at various locations and elevations within the soil box revealed a homogeneous profile with a medium-dense relative density of 50%. During the sand pluviation process, the pile was secured through temporary bracing to maintain its position in the center of the laminar box.

The pile material consisted of a polymer concrete, commercially available as Sikacrete 211 SCC Plus, with a measured compressive strength ($f'_c$) of 69 MPa (ASTM C39). Concrete cylinder testing allowed for back-calculation of an elastic modulus (E) of 29771 MPa. Splitting tensile testing revealed a tensile strength (f'sp) of 4.8 $kN/m^2$ (ASTM C496/C496M). The pile reinforcement consisted of Grade 60 A706 rebar. Longitudinal reinforcement consisted of 6-

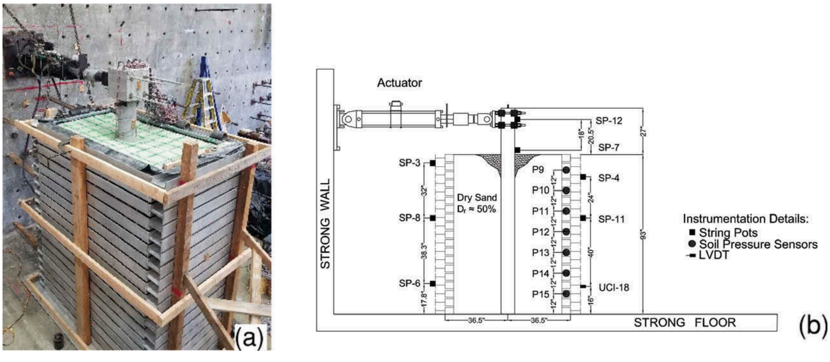


Figure 1. (a) Laminar soil box, (b) External instrumentation layout.

#3 bars ($A_{s,\ \#3}$ = 71 $mm^2$) arranged in even peripheral spacing around the circumference of the pile. Transverse reinforcement consisting of #3 hoops was placed at 20 cm vertical spacing. The longitudinal and transverse reinforcement ratios were determined to be ρl = 1.3% and ρt = 0.8%, respectively.

The test specimen was internally and externally instrumented with strain gauges, linear variable differential transducers (LVDTs), string potentiometers, and soil pressure sensors. Specifically, 22 strain gauges were attached to the vertical rebar in the push and pull direction and spaced every 15 cm from the bottom of the pile. Externally, i.e., above the soil surface, string potentiometers and LVDT's were attached to the pile specimen to measure the deflection under lateral loading. In addition, a series of string potentiometers monitored the movement of the restraint laminar soil box. Soil pressure sensors were placed along the container wall in push direction and spaced vertically every 30 cm. All sensors were connected to a National Instrument data acquisition system. An overview of the general test setup is presented in Figure 1(b).

### 2.2 *Loading protocol*

Quasi static reverse cyclic lateral loading was applied with a 650 kN capacity, 86 cm stroke hy-draulic actuator (Ortman 3TH, style G). The hydraulic actuator was controlled using a MTS Flextest GT controller and operated in displacement control. The loading protocol was guided by pre-test analytical studies using the software LPILE. In accordance with ASCE 41-06 S1, three loading cycles were applied at each displacement level. The range of displacements spanned from zero to +/- 17.8 cm.

### 2.3 *Test results*

Figure 2 shows the cyclic load-deflection relationships and backbone curve. The backbone curve was generated using the peak load values for each displacement level in push (positive) and pull (negative) direction. The maximum load in the push loading direction was measured to be 15 kN at 12.7 cm of displacement, whereas the maximum load observed in the pull direction was 16 kN at 8.9 cm of displacement. The maximum total displacement applied to the pile specimen was 17.5 cm in the push direction, and 17.8 cm in the pull direction.

## 3 BRIEF DISCUSSION ON TRADITIONAL P-Y CURVE DERIVATION

The traditional derivation process of p-y curves via strain gauges readings from laterally loaded pile tests commonly require five general steps:

Analyses and fitting of experimental curvature data obtained from pairs of strain gauges located at the same elevation:

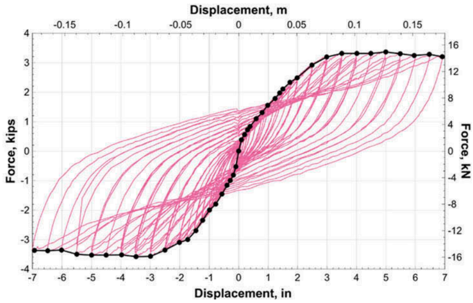


Figure 2. Experimentalload displacement relationship

$$\Phi(z) = \frac{d^2y}{dz^2} = \frac{\varepsilon_1(z) - \varepsilon_2(z)}{d} \quad (1)$$

where $\varepsilon_1$ and $\varepsilon_2$ are axial strainsrecordson opposites sides of the pile at elevation $z$, and $d$ is the horizontal distance between sensors.

2. Derivation of the pile deflections ($y$) with respect to the pile depth through double integration of curvature data and utilization of appropriate boundary conditions (e.g. known top or bottom pile displacements);
3. Determination of moment profiles along the pile depth by translating curvature data via nonlinear moment- curvature relationships into moment profiles
4. Data fitting of bending moment data by using known boundary conditions such as known moments at the ground surface
5. Derivation of soil resistance ($p$) versus the pile length by double differentiating moment profile.

The primary challenges related to the traditional p-y derivation process are associated with the integration and derivation procedures. While double integration of discrete data points tends to minimize the measurement errors of strain gauges and does not incur numerical errors, the double differentiation of discrete data points results in amplification of measurement errors and conse-quently inaccurate soil reactions (Yang & Liang (2006)). Several researchers proposed techniques to minimize numerical errors due to double differentiation of the moment data. The most commonly used methods include: regression techniques (e.g. Wilson (1998), Janoyan et al. (2001), Brandenberg et al. (2010), Yang et al. (2005)); numerical methods, such as high order global polynomial interpolations (e.g. Reese & Welch (1975)); piecewise polynomial curve fitting (e.g. Matlock & Ripperger (1956)); cubic spline fitting method (e.g. Dou & Byrne (1996)); and a combination of the first two methods (e.g. de Sousa Countinho (2006); Stewart et al. (2007)).

Each method has its own advantages and disadvantages, and the choice of the fitting method strongly depends on the data set at hand. Regression techniques work generally best with many data points available and are recommended only when data trends can be captured. Alternatively, reliable fitting functions for data sets with less data points could be captured with piecewise functions, such as piecewise polynomial functions and spline fitting techniques (e.g. B-spline). The result of this approach is a piecewise polynomial formulation that can be infinitely integrated and differentiated. The major drawback of a spline is its susceptibility to high frequency noise upon differentiation, since every point is fitted exactly (Wilson (1998)). This was also observed in the studies conducted by Stewart et al. (2007) and Lemnitzer et al. (2010), where a weighted residuals and B-spline approach were used to generate curvature and moment profiles. The results were found to be unstable because of the extreme sensitivity of the soil reaction profile to the subtle features of the curvature profile and the nonlinear moment-curvature relationship (Khalili-Tehrani et al. (2013)).

Several studies in current literature evaluate the numerous methodologies used for deducing *p-y* curves from lateral load test data and seek to recommend the most robust and accurate approach (e.g. Scott (1980), Wilson (1998), de Sousa Countinho (2006), Yang & Liang (2006), Brandenberg et al. (2010)). However, no conclusion has been reached to date, no universally applicable method has been found. Most available methods work well with one specific data set.

## 4 P-Y CURVES DERIVATION THROUGH GENETIC ALGORITHM

A pilot computational framework was developed to derive *p-y* curves using experimental data in the presence of both disturbed readings and pile nonlinearity. Parameters used to model the experimentally derived strains are optimized with respect to an objective function that considers the suitability of the fit to both, the strain and curvature data, as well as the resulting derived *p-y* curves. Genetic algorithms optimize a population of parameters through a process of selection borrowed from evolutionary biology. This parameter population is not confined to a single model. By carefully defining an objective function that considers the quality of a fit across several statistical models and parameter selections, a population may include any number of parameters for any number of possible models. This approach could enable a more robust generation of *p-y* curves from an ensemble of statistical methods that can be readily applied to any experimental dataset.

The genetic programming algorithm (GA) is a search heuristic based on the principles of genetics and natural selection (Goldberg (1989)). GA was first introduced by Holland (1975), and later developed by Goldberg (1989). This stochastic optimization algorithm selects fitter individuals among a population based on the principle of "survival of the fittest." After generations of selecting the fittest individuals, the search is guided towards a global maxima or minima of the parameter defined search space.

Genetic algorithms and machine learning (ML) have been applied successfully to many geotechnical engineering problems. ML techniques have been used in axially loaded piles design for ultimate bearing capacity' s prediction (e.g. Goh (1994), Goh et al. (2005), Shahin (2014)), settlement estimation (e.g. Nawari et al. (1999), Nejad et al. (2009)), and load-settlement response (e.g. Shahin (2014), Ismail and Jeng (2011), Alkroosh and Nikraz (2011)). There are very few studies showing application of ML techniques to laterally loaded piles. Ahangar-Asr et al. (2014) and Das and Basudhar (2006) used Artificial Neural Networks to predict lateral load capacity and then compared response predictions to analytical results from limit state models. Xue et al. (2006) us the GA concept to determine *p-y* curves in sand. However, their approach does not follow the traditional double differentiation of bending moment profiles to obtain the soil reaction, since their starting point is the assumption that the soil reaction can be fit by a fourth order polynomial equation.

A genetic algorithm comprises of six parts:

1. Generation of a random population: The parameters are coded into random strings.
2. Evaluation of the fitness of each solution string: An objective function is used to measure the accuracy of each fitting.
3. Selection: Individuals with higher fitness value have a higher probability of being selected and producing offspring in the next generation. At each iteration, the algorithm evaluates each string by returning a resulting score from the objective function. The top 10% of parameter strings are selected by score and used to generate the next population of strings.
4. Crossover: Two individual strings chosen from the population are combined to form a new string in the next population.
5. Mutation: Each parameter in every new string in the next population has a 10% chance of being replaced by a random value within the input parameter distribution.
6. Termination: The search algorithm concludes when the change in average fitness for the next population falls under a threshold.

The result of any optimization is entirely dependent on the function and parameters to be optimized. The objective function should accurately characterize the properties of realistic *p-y* curves to effectively narrow down a single solution. Specifically, resulting *p-y* curves need to be both monotonically increasing and depth dependent.

The proposed GA framework to obtain *p-y* curves from the data available in this experiment is shown in Figure 3. The GA begins with the generation of 200 strings; each representing input parameters for curvature and moment at 26 separate deflections levels. 13 positive and 13 negative deflections ranging from +/- 0.5 cm to +/- 5 cm are considered in this algorithm. Eq. 3 shows the representation of each string in the population.

$$GA = [w_{c1}t_{c1}k_{c1}s_{c1}F_{c1}w_{m1}t_{m1}k_{m1}s_{m1}F_{m1}, \ldots, w_{ci}t_{ci}k_{ci}s_{ci}F_{ci}w_{mi}t_{mi}k_{mi}s_{mi}F_{mi}] \tag{2}$$

Where $w$ is the weight at data location, $t$ is the knots location, $k$ is the polynomial order, $s$ is the smoothing factor, and $F$ is the fitting function. The fitting models taken into consideration include the univariate, least square, and B- Spline methods. The first generation of strings is then double integrated and differentiated to obtain a series of *p-y* curves at various pile depths.

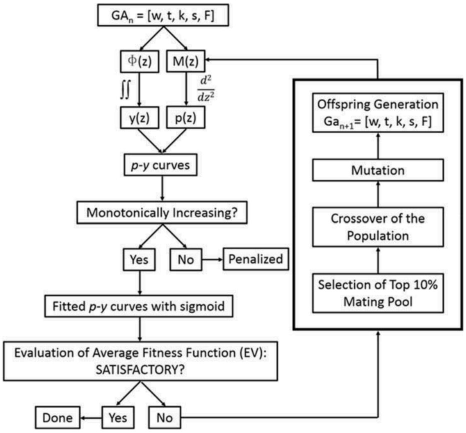


Figure 3. Genetic algorithm's process.

The *p-y* estimates for a given input string must be monotonically increasing provided that an increase of soil reaction corresponds to an increase of deflection. If this condition is not met, the string is heavily penalized by the objective function. Finally, the resulting estimates need to be fitted to a final *p*- y curve. The chosen fitted function was a sigmoid, which is monotonic and constrained by a pair of horizontal asymptotes as *x*. The sigmoid function can be expressed as:

$$f(x) = \frac{y_{\max}}{1 + e^{-x}} \tag{3}$$

where $y_{max}$ represents the upper bound of the sigmoid. The fitness function evaluates the explained variance between the raw and fitted *p-y* curves and is represented by the minimization of the following score function:

$$Score = \sum\nolimits_{z=1}^{m} EV_z, \tag{4}$$

where $EV_z$ is the explained variance, and z is the number of depths considered in the analysis.

### 4.1 *Discussion on GA p-y curves*

Figures 4 a&b present sample *p-y* relationships derived using the GA procedure described above. The curves depicted in Figure 4a correspond to soil reactions at depths between -51 cm and -178 cm below ground surface. The *p-y* data obtained through the GA were fitted with a sigmoid function. Note that the presented data correspond to measurements recorded in pull direction (i.e., negative deflections). For this specific dataset, the preferred interpolation technique was the UNIvariate method, where the knots' location was dictated by the smoothing factor. This ensured curvature and especially moment data to be fitted using profiles without many local extrema. It was found that the proposed method predicted a realistic soil reaction profile and *p-y* curves. The results indicated that the second order polynomial only provided a satisfactory description of the soil reaction profile.

The generated *p-y* curves, were also compared to traditional *p-y* relationships as shown in Figure 4b. The results show that the traditional method (e.g. Reese et al. (1974)), which was derived for 0.6 m diameter driven piles does not align with the results obtained through the GA procedure for this experiment. A certain mismatch was expected given the specific soil and boundary conditions that both *p-y* relationships were derived for. While upscaling is known to underestimate the soil reaction and lateral capacity of pile foundations (e.g., by utilizing the relationships for large diameter piles), downscaling is less researched in literature. Yet, the reduction of available surface area for side friction and frontal contact pressure is

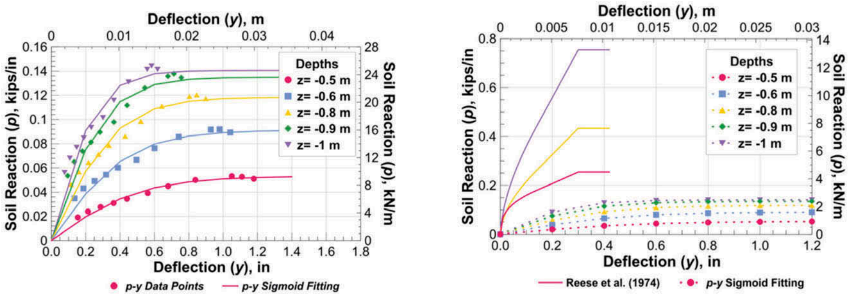


Figure 4. Figure 4a&b. Experimental and fitted *p-y* curves obtained from the GA at various depths (left); and comparison between experimental GA *p-y* curves and analytically formulations (right).

smaller for small diameter piles and should therefore generate less contact for soil resistance. As indicated in Figure 4b, the experimental *p-y* curves obtained for the 20 cm pile exhibit a smaller ultimate soil reaction than Reese et al. (1974)' s relationships. In addition, Reese et al.'s *p-y* curves are also significantly stiffer in both directions (Figure 4b). This difference can potentially be amplified by the nature of the *p-y* derivation. While analytical *p-y* curves are a function of the modulus of subgrade reaction, an intrinsic property of the soil subject to the accuracy of the in-situ investigation, GA *p-y* curves are derived using curvature measurements taken from strain gauges installed inside the pile directly. While strain measurements are also subject to the accuracy of the sensor instrumentation and expertise of the researcher, this methodology might however capture more the structural bending behavior than the geotechnical component in the soil-structure interaction problem.

## 5 SUMMARY

A model scale lateral load test on a 20 cm diameter reinforced concrete pile was used to develop a pilot genetic algorithm (GA) framework for the derivation of *p-y* formulations. This approach has the potential to overcome current challenges associated with experimental *p-y* curves derivation pertaining to the choice of fitting technique and input model parameters. A GA approach allows the generation of *p-y* curves from different statistical methods, ensuring the best solution across many variables and methods, and ideally, is applicable to any experimental data set. Sample GA-derived *p-y* relationships are presented for depths of -51 cm to -178 cm. The *p-y* data were fitted with a sigmoid function and are extrapolated to other depths. Comparison with formulations from literature indicated that the lateral soil resistance in the experiment was less than the predicted capacity and more flexible in terms of initial soil stiffness.

## REFERENCES

A. Ahangar-Asr, A.A. Javadi, A. Johari, and Y. Chen. Lateral load bearing capacity modelling of piles in cohesive soils in undrained conditions: An intelligent evolutionary approach. Applied Soft Computing, 24:822–828, 2014.

E.R. Ahlberg. Interaction between soil and full scale drilled shafts under cyclic lateral loads. University of California, Los Angeles, 2008.

I. Alkroosh and H. Nikraz. Correlation of pile axial capacity and cpt data using gene expression programming. Geotechnical and Geological Engineering, 29(5):725–748, 2011.

API. 2a-wsd. Recommended Practice for Planning, Designing and Constructing Fixed Offshore Platforms-Working Stress Design, 21, 2000.

ASCE/SEI Seismic Rehabilitation Standards Committee. "Seismic rehabilitation of existing buildings (ASCE/SEI 41-06)". American Society of Civil Engineers, Reston, VA (2007).

ASTM. Standard practice for the use of the international system of units (SI) (the modernized metric system). In E 380-91a. ASTM, Philadelphia, Pa., 1991.

E.C. Bentz. Sectional analysis of reinforced concrete members. University of Toronto Toronto, 2000.
S.J. Brandenberg, D.W. Wilson, and M.M. Rashid. Weighted residual numerical differentiation algorithm applied to experimental bending moment data. Journal of Geotechnical and Geoenvironmental Engineering, 136(6):854–863, 2010.
S.K. Das and P.K. Basudhar. Undrained lateral load capacity of piles in clay using artificial neural network. Computers and Geotechnics, 33(8):454–459, 2006.
A.G. de Sousa Coutinho. Data reduction of horizontal load full-scale tests on bored concrete piles and pile groups. Journal of Geotechnical and Geoenvironmental Engineering, 132(6):752–769, 2006.
H. Dou and P.M. Byrne. Dynamic response of single piles and soil pile interaction. Canadian Geotechnical Journal, 33(1):80–96, 1996.
A.T.C. Goh, F.H. Kulhawy, and C.G. Chua. Bayesian neural network analysis of undrained side resistance of drilled shafts. Journal of Geotechnical and Geoenvironmental Engineering, 131(1):84–93, 2005.
A.T.C. Goh. Nonlinear modelling in geotechnical engineering using neural networks. Transactions of the Institution of Engineers, Australia. Civil engineering, 36(4):293–297, 1994.
D. Goldberg. Genetic algorithms in optimization, search and machine learning. Addison-Wesley, 1989.
A. Ismail and D. Jeng. Modelling load–settlement behaviour of piles using high-order neural network (hon-pile model). Engineering Applications of Artificial Intelligence, 24(5):813–821, 2011.
K. Janoyan, J.P. Stewart, and J.W. Wallace. Analysis of py curves from lateral load test of large diameter drilled shaft in stiff clay. In Proceedings of the 6th Caltrans workshop on seismic research, Sacramento, CA, 2001.
H.J. Holland. 1975. adaptation in natural and artificial systems. Ann Arbor: University of Michigan Press.
P. Khalili-Tehrani, E.R. Ahlberg, C. Rha, A. Lemnitzer, J.P. Stewart, E. Taciroglu, and J.W. Wallace. Nonlinear load-deflection behavior of reinforced concrete drilled piles in stiff clay. Journal of Geotechnical and Geoenvironmental Engineering, 2013.
A. Lemnitzer, P. Khalili-Tehrani, E.R. Ahlberg, C. Rha, E. Taciroglu, J.W. Wallace, and J.P. Stewart. Nonlinear efficiency of bored pile group under lateral loading. Journal of geotechnical and geoenvironmental engineering, 136(12):1673–1685, 2010.
H. Matlock. Correlations for design of laterally loaded piles in soft clay. Offshore Technology in Civil Engineering Hall of Fame Papers from the Early Years, pages 77–94, 1970.
H. Matlock and L.C. Reese. Generalized solutions for laterally loaded piles. Journal of the Soil Mechanics and Foundations Division, 86(5):63–94, 1960.
H. Matlock and E.A. Ripperger. Procedures and instrumentation for tests on a laterally loaded pile. In Proceedings, Eighth Texas Conference on Soil Mechanics and Foundation Engineering, 1956.
B. McClelland and J.A. Focht. Soil modulus for laterally loaded piles. Transactions of the American Society of Civil Engineers, 123(1):1049–1063, 1958.
N.O. Nawari, R. Liang, and J. Nusairat. Artificial intelligence techniques for the design and analysis of deep foundations. Electronic Journal of Geotechnical Engineering, 4:1–21, 1999.
F. Nejad, M. BJaksa, M. Kakhi, and B.A. McCabe. Prediction of pile settlement using artificial neural networks based on standard penetration test data. Computers and Geotechnics, 36(7):1125–1133, 2009.
L.C. Reese, W.R. Cox, and F.D. Koop. Analysis of laterally loaded piles in sand. Offshore Technology in Civil Engineering Hall of Fame Papers from the Early Years, pages 95–105, 1974.
L.C. Reese and R.C. Welch. Lateral loading of deep foundations in stiff clay. Journal of the Geotechnical engineering division, 101(7):633–649, 1975.
R. F. Scott. Analysis of centrifuge pile tests; simulation of pile-driving. 1980.
M.A. Shahin. Intelligent computing for modeling axial capacity of pile foundations. Canadian Geotechnical Journal, 47(2):230–243, 2010.
M.A. Shahin. Load–settlement modeling of axially loaded steel driven piles using cpt-based recurrent neural networks. Soils and Foundations, 54(3):515–522, 2014.
J.P. Stewart, E. Taciroglu, J.W. Wallace, E.R. Ahlberg, A. Lemnitzer, C. Rha, P. Tehrani, S. Keowen, R.L. Nigbor, and A. Salamanca. Full scale cyclic testing of foundation support systems for highway bridges. part ii: Abutment backwalls. UCLA Structural and Geotechnical Engineering Laboratory, (UCLA-SGEL 2007/02), 2007.
D.W. Wilson. Soil-pile-superstructure interaction in liquefying sand and soft clay. PhD thesis, Citeseer, 1998.
E. Winkler. Theory of elasticity and strength. Dominicus Prague, Czechoslovakia, 1867.
J. Xue, K. Gavin, G. Murphy, P. Doherty, and D. Igoe. Optimization technique to determine the py curves of laterally loaded stiff piles in dense sand. Geotechnical Testing Journal, 39(5):842–854, 2016.
K. Yang and R. Liang. Methods for deriving py curves from instrumented lateral load tests. 2006.
K. Yang, R. Liang, S Liu. Analysis and test of rock-socketed drilled shafts under lateral loads. In Alaska Rocks 2005, The 40th US Symposium on Rock Mechanics (USRMS). American Rock Mechanics Association, 2005.